Crystallization Kinetics and Morphology of Binary Phenolic/Poly(ϵ-caprolactone) Blends

SHIAO-WEI KUO, SHIH-CHI CHAN, FENG-CHIH CHANG

Institute of Applied Chemistry, National Chiao Tung University, Hsin Chu, Taiwan

Received 9 March 2003; revised 6 June 2003; accepted 19 June 2003

ABSTRACT: For the first time, quantitative analyses of the crystallization kinetics, surface free energy of chain folding, and morphology in phenolic/poly(ϵ-caprolactone) (PCL) binary blends have been studied. The spherulite growth rate and the overall crystallization rate depend on the crystallization temperature and PCL content in the blend. In addition, the crystallization and melting temperatures of the PCL phase decrease with an increase in the phenolic content. An Avrami analysis shows that the addition of phenolic to PCL results in a decrease in the overall crystallization rate of the PCL phase. The presence of an amorphous phenolic phase results in a reduction in the rate of the spherulite growth of PCL. The surface free energy of folding increases with increasing phenolic content, and the crystal thickness of a phenolic/PCL blend, according to small-angle X-ray scattering (SAXS), is greater than that of pure PCL because of the increase in the surface free energy of chain folding and the decrease in the degree of supercooling. The observed domain size of the crystalline/amorphous phase (5.9 nm) from SAXS is also consistent with that from solid-state NMR (3–20 nm). All these results indicate that the crystallization ability of PCL decreases with increasing phenolic content in the blends. © 2003 Wiley Periodicals, Inc. J Polym Sci Part B: Polym Phys 42: 117–128, 2004

Keywords: crystallization kinetics; morphology; hydrogen bonding; blending; SAXS

INTRODUCTION

The crystallization kinetics and morphology of miscible binary blends of amorphous/crystalline polymers have widely been studied.[1–9] Generally, a depression of the growth kinetics of the crystallizable component has been found with the addition of the amorphous component because of the reduction in the chain mobility, the dilution of the crystallizable component at the growth front, the change in the free energy of nucleation as a result of a specific interaction, and the morphology of the amorphous/crystallization binary blend competition between the advancing spherulite front and the diffusion of the amorphous component into interlamellar and interfibrillar regions. However, the crystallization kinetics of miscible polymer blends through hydrogen bonding has received relatively less attention, in part because of the inherent complexity of such mixtures.[10,11]

Poly(ϵ-caprolactone) is a highly crystalline polymer that is miscible with several amorphous polymers that have been discussed previously.[12] DeJuana and Cortazar[13] studied the crystallization kinetics and melting behavior of phenoxy/PCL blends, showing that the PCL chain folding surface free energy in the blend with phenoxy was lower than that of pure PCL. In general, the crystallization kinetics and the related microstructure of a crystalline blend depend on the intermo-

Correspondence to: F.-C. Chang (E-mail: changfc@cc.nctu.edu.tw)

Journal of Polymer Science: Part B: Polymer Physics, Vol. 42, 117–128 (2004)

lecular interaction of the diluent amorphous phase and its glass-transition temperature (T_g).

We have studied the miscibility behavior in phenolic/PCL blends[14] as fully miscible blends because of the formation of intermolecular hydrogen bonding between the hydroxyl group of phenolic and the carbonyl group of PCL and a negative value of the polymer–polymer interaction energy density (B) based on the Nish–Wang equation.[15] In addition, the interassociation equilibrium constant for phenolic/PCL blends is higher than the self-association equilibrium constant of PCL based on the Painter–Coleman association model,[16] and this suggests that the tendency toward hydrogen bonding of phenolic and PCL is more favorable than intramolecular hydrogen bonding of phenolic in the mixture. Zhong et al.[17] reported a single, composition-dependent spin–lattice relaxation in the laboratory frame [$T_1(H)$] but two spin–lattice relaxation times in the rotating frame [$T_{1\rho}(H)$] in a phenolic/PCL blend system. This indicates that the domain size of the PCL crystalline/amorphous phase is less than the $T_1(H)$ measured scale of 20–30 nm but larger than the $T_{1\rho}(H)$ measured scale of 2–3 nm. However, the exact thickness of the crystalline phase in phenolic/PCL blends is still not fully understood.

In this study, the crystallization kinetics, surface free energy of chain folding (σ_e), and thickness of the crystalline phase in phenolic/PCL blends have been investigated with differential scanning calorimetry (DSC), optical microscopy, and small-angle X-ray scattering (SAXS), respectively.

EXPERIMENTAL

Materials

PCL used in this study was TONE polymer P-787 purchased from Union Carbide Corp.; it had a number-average molecular weight of 80,000 g/mol. The phenolic was synthesized with sulfuric acid via a condensation reaction and had a number-average molecular weight of 500 and a weight-average molecular weight of 1200 g/mol.

Blend Preparation

The solution blending of phenolic/PCL blends of various compositions was performed in a tetrahydrofuran solution containing a total of 5 wt % polymer. The polymer blend solution was stirred for 6–8 h, and the solution was allowed to evaporate slowly at room temperature for 1 day. The film of the blend was then dried at 50 °C for 2 days for the removal of the residual solvent.

Characterization

DSC

The melting and crystallization behavior and T_g of the polymer blends were studied by DSC with a DuPont DSC-9000 instrument. T_g was determined at a scan rate of 20 °C/min and within a temperature range of 30–80 °C. Approximately 5–10 mg of each blend was weighed and sealed in an aluminum pan. The sample was quickly cooled to −100 °C from the melt of the first scan and scanned between −100 and 250 °C at 20 °C/min. T_g is at the midpoint of the specific heat increment. The crystallization temperature (T_c) was determined by the cooling of the melt at 80 °C at a cooling rate of −10 °C/min. We also used DSC to study the kinetics of isothermal crystallization by rapidly cooling a sample to T_c from the melt at 80 °C for 10 min and then keeping it at T_c for 12 h. The crystallinity is expressed as the ratio of the peak area at some time to that at the end of crystallization. After the isothermal crystallization was completed, the sample was cooled to 0 °C and then heated to 100 °C at a heating rate of 10 °C/min for the measurement of the melting temperature (T_m).

Optical Microscopy

The spherulite growth rate was determined with a polarized light microscope manufactured by Olympus Limited Co. (Japan) and equipped with a heating stage (Mettler FP90) and was photographed with a CCD camera. Each sample was sandwiched between two thin glass slides, melted for 10 min on a hot stage at 80 °C, and then transferred as quickly as possible onto another hot stage preheated to the desired T_c. The samples were crystallized isothermally at a given T_c to monitor the growth of the spherulite as a function of time. The radial growth rate of the PCL spherulite was calculated as the slope of the line obtained from a plot of the spherulitic radius versus time. Furthermore, the phase-separation phenomenon was also detected by optical microscopy by the heating of the blend at 80 °C under a nitrogen atmosphere (to avoid thermal degrada-

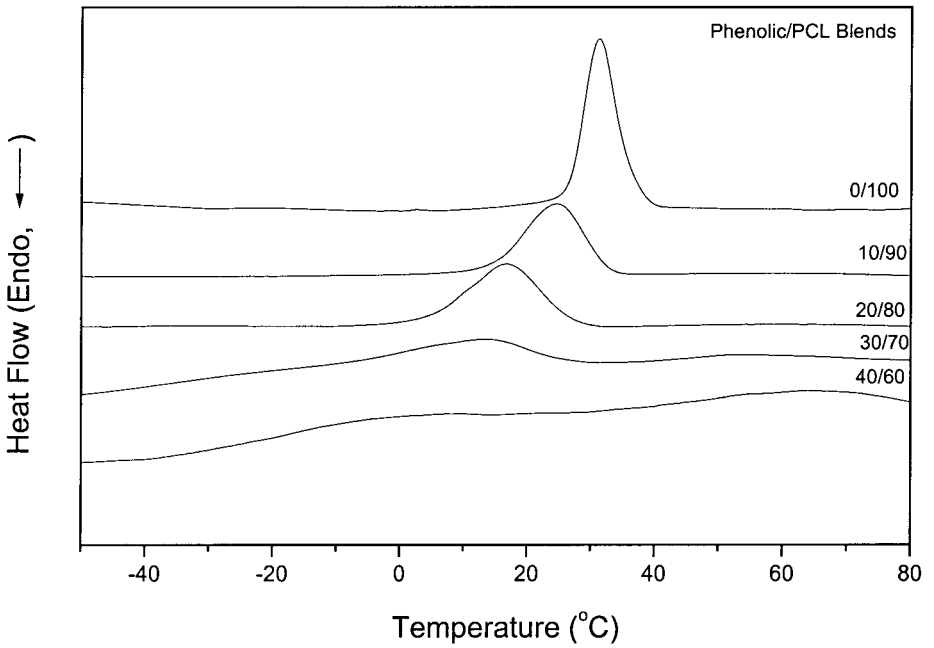

Figure 1. DSC scans of phenolic/PCL blends with different compositions at a cooling rate of −10 °C/min from 80 to −50 °C.

tion) and subsequent heating from 80 to 250 °C at a rate of 1 °C/min.

SAXS Measurements

All SAXS measurements were performed at room temperature. The power of the X-ray source was operated at 200 mA and 40 kV. The X-ray source was a 18-kW rotating-anode X-ray generator equipped with a rotating-anode Cu target. The incident X-ray beam was monochromated with pyrolytic graphite, and a set of three pinhole inherent collimators was used so that the smearing effects inherent in slit-collimated small-angle X-ray cameras could be avoided. The sizes of the first and second pinholes were 1.5 and 1.0 mm, respectively, and the size of the guard pinhole before the sample was 2.0 mm. The scattered intensity was detected with a two-dimensional position-sensitive detector (Ordela 2201X, Oak Ridge Detector Laboratory, Inc.) with 256 × 256 channels. The sample-to-detector distance was 4000 mm. The beam stop was around a lead disk 18 mm in diameter. All data were corrected by the background and the sensitivity of each pixel of the area detector. The area scattering pattern was radically averaged to increase the efficiency of data collection in comparison with a one-dimensional linear detector.

RESULTS AND DISCUSSION

Miscibility, Crystallization, and Melting Behavior Analysis

In our previous study,[14] we found that the phenolic/PCL blend system is a totally miscible blend system because only a single T_g was detected on the DSC thermograms. In addition, the miscibility diagram was predicted within −25 to 300 °C on the basis of the Painter–Coleman association model. This result is consistent with that from optical microscopy observations: no phase separation occurs by the heating of the blend from room temperature to 250 °C. Therefore, the phenolic/PCL blend is miscible from room temperature to 250 °C for all compositions. Figure 1 shows the cooling DSC thermograms of pure PCL and various phenolic/PCL compositions at a cooling rate of −10 °C/min from 80 to −50 °C. T_c of the PCL component in the blend decreases significantly with an increase in the phenolic content in comparison with that of pure PCL. The exothermic peak of PCL crystallization disappears for the 40/60 phenolic/PCL blend, and this suggests that the phenolic component retards or even inhibits the PCL crystallization in the phenolic/PCL blend. In addition, Figure 2 shows the DSC heating thermograms of pure PCL and various phe-

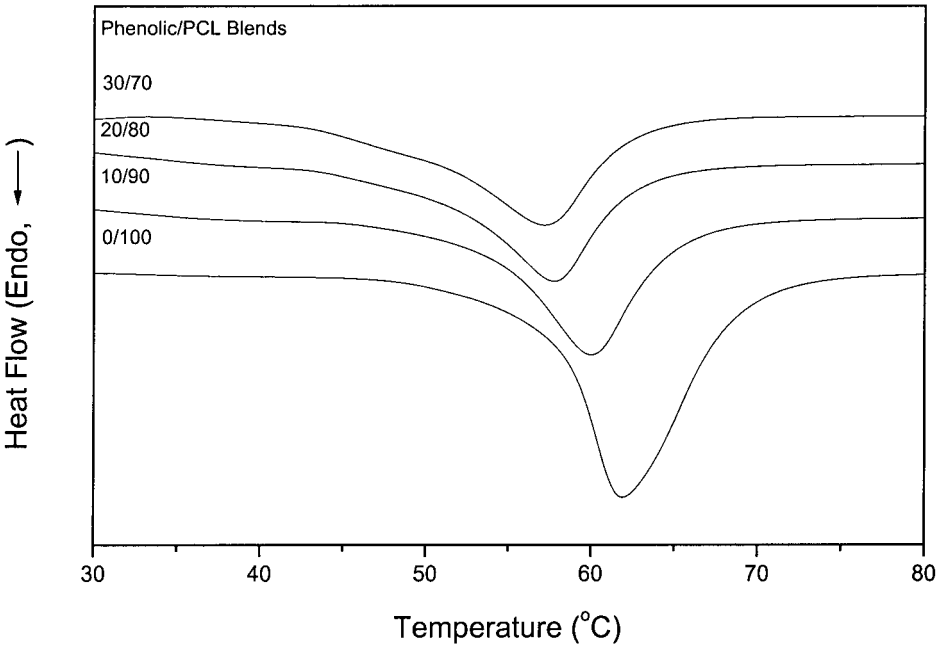

Figure 2. DSC scans of phenolic/PCL blends with different compositions at a heating rate of 10 °C/min from 30 to 80 °C

nolic/PCL blends after the isothermal T_c (40 °C) was maintained for 12 h. T_m of the PCL component in the blend decreases with an increase in the phenolic content. A melting point depression is characteristic of a miscible polymer blend in a melting state, in which thermodynamic equilibrium is nearly approached under the performed process. In fact, a negative value of B of the phenolic/PCL system was calculated in our previous study, and this implies that the phenolic/PCL system is miscible in the melt state.

Isothermal Crystallization Kinetics

Figure 3 shows typical isotherms by plotting the relative crystallinity [i.e., the weight fraction of the material crystallized after time t (X_t)] against time for different phenolic/PCL compositions at T_c = 40 °C. From these curves, the half-time of crystallization ($t_{1/2}$) is defined as the time required for half of the final crystallinity to be developed. Figure 4 plots $t_{1/2}$ versus T_c for pure PCL and various phenolic/PCL blends, indicating that the overall crystallization rate decreases with an increase in phenolic contents at constant T_c.

The crystallization kinetics of the pure PCL and phenolic/PCL blends have been analyzed with the Avrami treatment:[18]

$$\log[-\ln(1 - X_t)] = \log k + n\log(t) \qquad (1)$$

where n is the Avrami exponent, which depends both on the nature of the primary nucleation and on the growth geometry of the crystalline entities, and k is the overall kinetic rate constant, which depends on the rates of nucleation and growth. k and n can be calculated from the intercept and slope of eq 1. Figure 5 shows the linear relationship between $\log[-\ln(1 - X_t)]$ and $\log t$ of the 10/90 phenolic/PCL blend at various T_c's. The values of k, n, and $t_{1/2}$ are summarized in Table 1. The values of n are not integers in almost all cases because of mixed growth or surface nucleation modes. The values of k decrease with increasing phenolic content and T_c. The same trend was also observed for a phenoxy/PCL blend system.[13] It is well known that the molecular mobility is the controlling factor at a low T_c, whereas at a high T_c, the process is controlled by nucleation, so that k decreases with increasing T_c.

Spherulite Growth Kinetics

Spherulite growth kinetics in miscible blends of crystalline/amorphous polymers have been reported.[19–22] The Lauritzen–Hoffman theory has widely been employed to study the crystallization

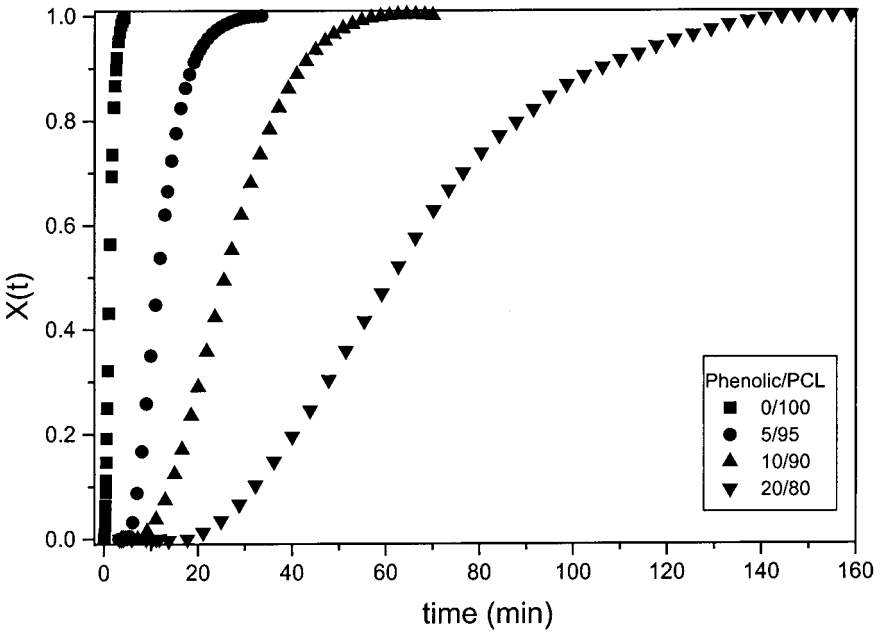

Figure 3. Crystallization isotherms of phenolic/PCL blends at 40 °C.

kinetics in miscible blends of crystalline/amorphous polymers.[23] In this study, the spherulite growth rates of phenolic/PCL blends have been determined with a polarizing optical microscope. For brevity, Figure 6 gives plots of the spherulite radius versus time for various phenolic/PCL compositions crystallized at 40 °C. The solid lines represent the best least-square fit to the data. It is clear that there is a linear increase in the radius with time until the spherulite impinges on others. The slope of the line decreases with increasing phenolic content, as shown in Figure 6.

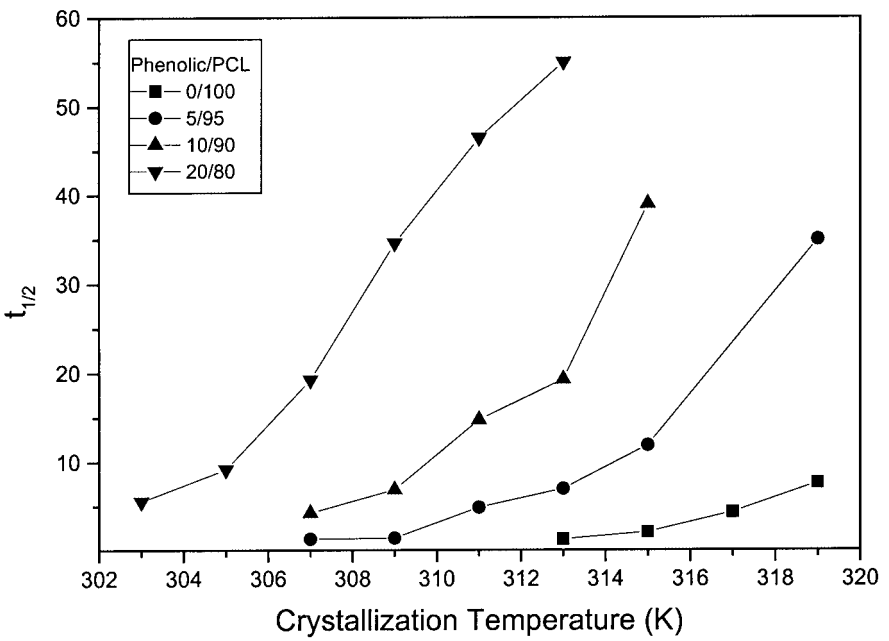

Figure 4. Plot of $t_{1/2}$ versus T_c for samples of different compositions of phenolic/PCL blends.

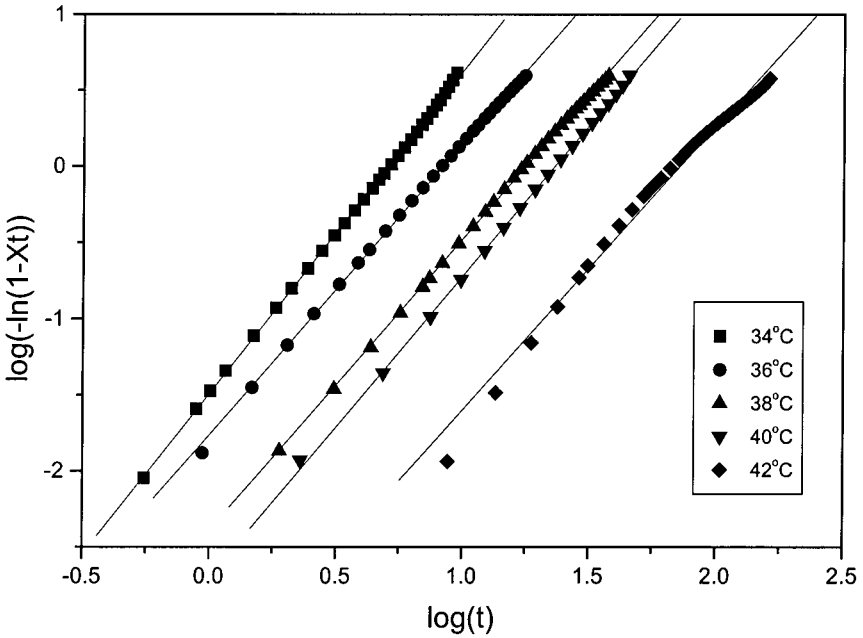

Figure 5. Avrami plot for a 10/90 phenolic/PCL blend at different T_c's.

Figure 7 plots the crystallization radial growth rate (G) versus T_c for pure PCL and various phenolic/PCL blends; the spherulite growth rate decreases with increasing phenolic content at a given T_c. The presence of amorphous phenolic with a high T_g in the blends significantly decreases the rate of PCL crystallization. Furthermore, the spherulite growth rate decreases with increasing T_c. In general, there are three main factors affecting the crystallization rate depression in the miscible crystalline/amorphous polymers with high T_g's: (1) the decrease in the segmental mobility of the crystalline polymer transporting across the liquid–solid interface due to the high T_g's of the blends, (2) the dilution effect that reduces the number of crystallizable segments on the front of the growth spherulite, and (3) the decrease in the supercooling due to the melting point depression.

Table 1. Values of k, n, $t_{1/2}$ as a Function of Composition, and T_c for Phenolic/PCL Blends

Phenolic/PCL	T_c (K)	n	k ($\times 10^3$)	$t_{1/2}$ (min)
0/100	313	2.8	441.8	1.3
	315	2.7	198.9	2.1
	317	2.7	95.4	4.4
	319	2.8	18.2	7.6
5/95	307	2.9	408.7	1.3
	309	2.7	390.1	1.4
	311	2.8	38.5	4.9
	313	2.7	23.2	7.0
	315	2.7	10.1	11.9
	319	3.0	0.8	35.0
10/90	307	3.1	32.3	4.3
	309	2.9	17.3	6.9
	311	2.9	4.1	14.8
	313	3.0	1.9	19.3
	315	2.9	0.8	39.7
20/80	303	2.8	32.0	5.6
	305	2.7	14.9	9.2
	307	2.5	7.5	19.3
	309	2.4	4.3	34.6
	311	2.5	2.1	46.5
	313	2.7	1.2	55.1

The Lauritzen–Hoffman model has been used to analyze the spherulite crystallization behavior of homopolymers and some crystalline/amorphous polymer blends. This theory has also been adopted to analyze the spherulite crystallization behavior of the phenolic/PCL blends in this study:

$$G = G_0 \exp\left[\frac{-U^*}{R(T - T_\infty)}\right] \exp\left[\frac{-K_g}{fT\Delta T}\right] \qquad (2)$$

where G_0 is the front factor, U^* is the activation energy for the segment diffusion to the site of

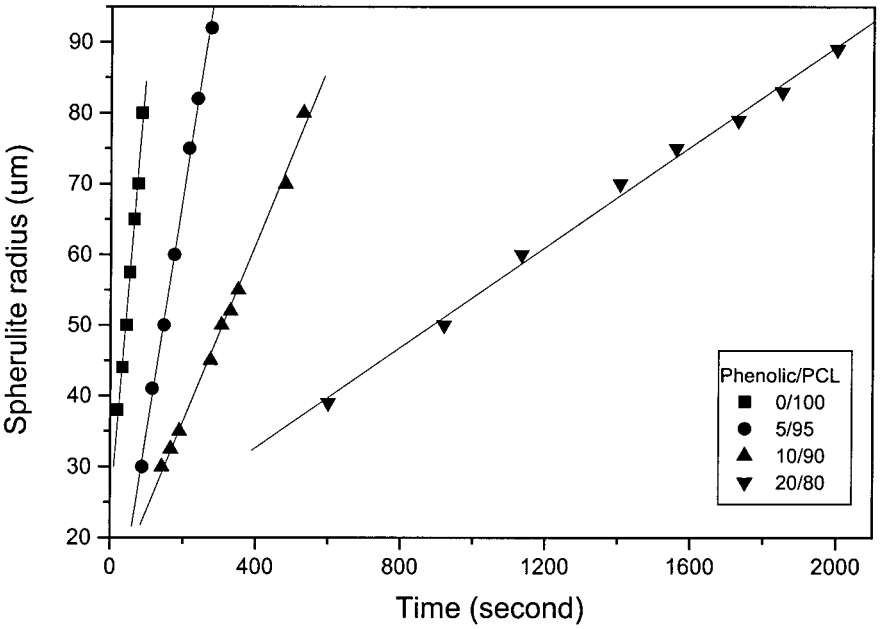

Figure 6. Spherulite radius as a function of time for phenolic/PCL blends with various compositions isothermally crystallized at 40 °C.

crystallization, R is the gas constant, T_∞ is the hypothetical temperature below which all viscous flow ceases, K_g is the nucleation parameter, ΔT is the degree of supercooling defined by $T_m^0 - T_c$ (where T_m^0 is the equilibrium melting temperature), and f is a correction factor given as $2T_c/(T_m^0 + T_c)$. It is important to emphasize that the parameters U^* and T_∞ are treated as variables to maximize the quality of the fit to eq 2. In this study, the Williams–Landel–Ferry (WLF) values of $U^* = 4120$ cal/mol and $T_\infty = T_g - 51.6$ are used.[24] K_g is given by[23–25]

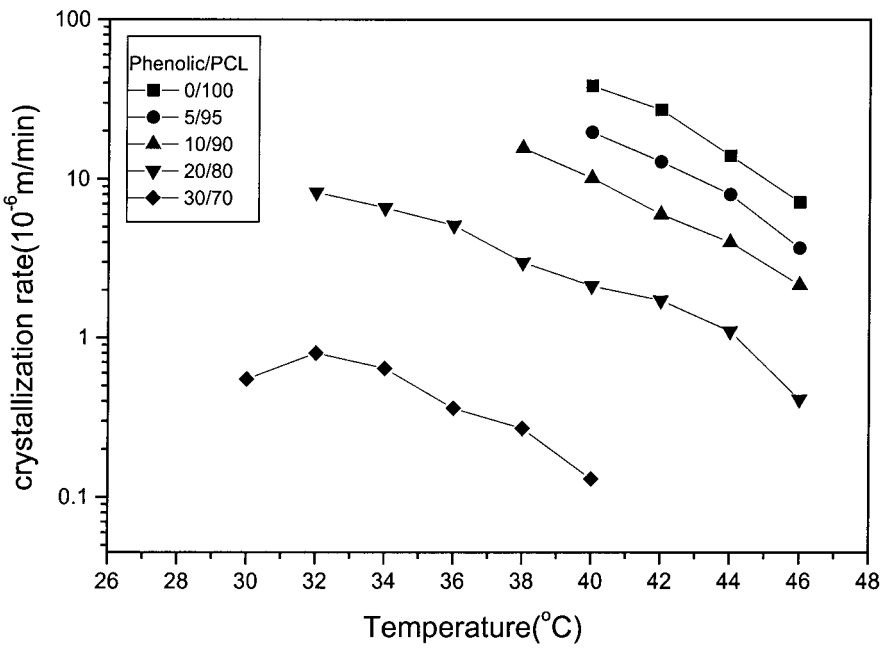

Figure 7. G as a function of T_c for phenolic/PCL blends.

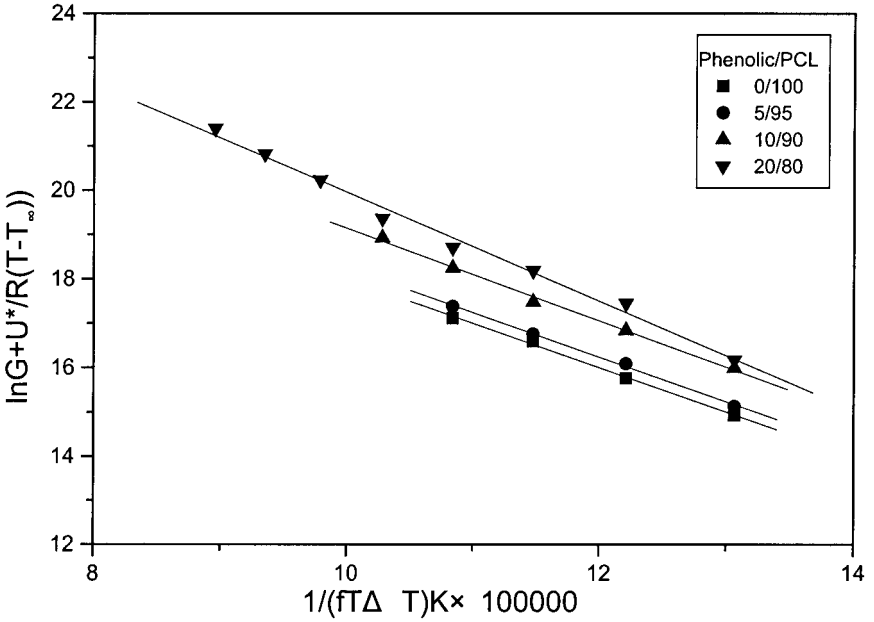

Figure 8. Kinetics analysis of crystallization rate constant data with WLF constants.

$$K_g = \frac{nb\sigma\sigma_e T_m^0}{\Delta h_f k_B} \quad (3)$$

where b is the thickness of a monomolecular layer; σ is the lateral surface free energy, Δh_f is the heat of fusion per unit of volume, and k_B is Boltzmann's constant. Typically, $n = 4$ is used in regimes I and III, but $n = 2$ in regime II has been employed. It is often most convenient to rearrange eq 2 as follows

$$\ln G + \frac{U^*}{R(T - T_\infty)} = \ln G_0 - \frac{K_g}{T(\Delta T)f} \quad (4)$$

and view the growth rate data in the form of a plot of the left-hand side of eq 4 versus $1/T_c(\Delta T)f$, with a slope equal to $-K_g$. Figure 8 shows such plots according to eq 4, and the K_g values obtained are summarized in Table 2. In this study, the regime is assigned to be regime II at about 30–40 °C.[13] The derived K_g values can be used to calculate σ_e and the work of chain folding (q) for PCL. With b = 0.412 nm,[26] T_m^0 = 70.9 °C,[14] and Δh_f = 1.63 × 10^9 erg/cm^3,[27] as previously determined, σ can be estimated with the Thomas–Stavely relationship:[28]

$$\sigma = \alpha b_0(\Delta h_f) \quad (5)$$

where α is an empirical constant that is usually assumed to be 0.1 for vinyl polymers and 0.25 for high-melting polyesters.[29] A low-T_m polyester such as PCL has a long run of CH_2 groups like polyethylene (PE), and a value of 0.1 is recommended. The value of σ_e for pure PCL is 72.36 erg/cm^2, which agrees well with a previously reported value.[13] The values of K_g(II) and σ_e for various blend compositions are also listed in Table 2. Both values increase with the increase in the phenolic content, and this indicates that the crystallization ability of PCL decreases with increasing phenolic content in the blend. The same trend of σ_e was also observed in a phenolic/poly(ethylene oxide) (PEO) blend system, in which σ_e increased with increasing phenolic content in the blend.[30] However, decreasing σ_e with increasing phenoxy content in a phenoxy/PCL blend system

Table 2. Comparison of σ_e and q for Phenolic/PCL Blends

Compositions	K_g (II) × 10^{-4} (deg^2)	σ_e (erg/cm^2)	q (kcal/mol)
0/100	9.9	72.36	3.93
5/95	10.0	72.68	
10/90	10.4	75.48	
20/80	12.2	88.96	
30/70	13.3	96.56	

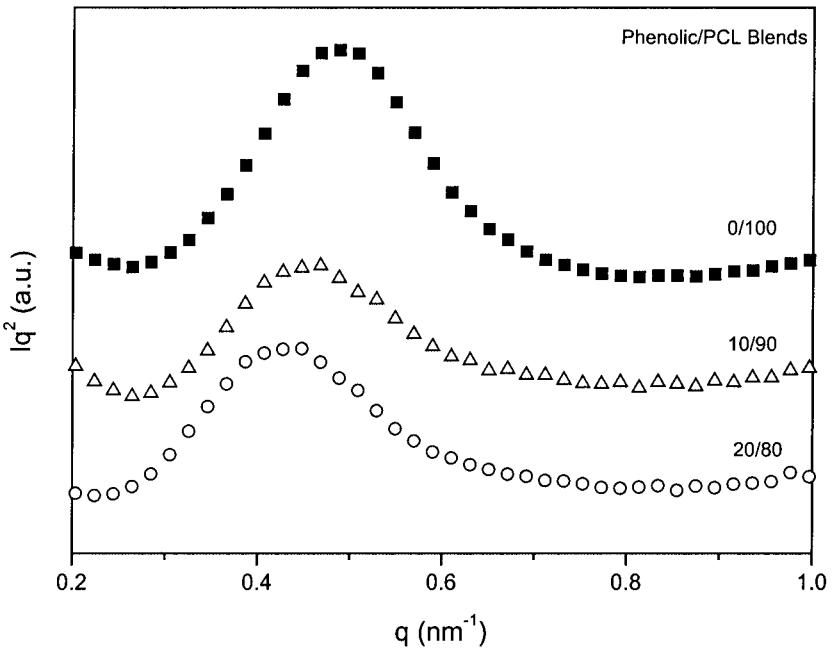

Figure 9. Profiles of Lorentz-corrected SAXS intensities of phenolic/PCL blends

was observed.[13] In our previous study,[31] we found that the interassociation equilibrium constants from both phenolic/PEO and phenolic/PCL blend systems were greater than the self-association equilibrium constant of pure phenolic; this indicated that hydrogen bonding was favored on intermolecular hydrogen bonding. On the contrary, the interassociation equilibrium constant (K_A) of the phenoxy/PCL blend system was lower than the self-association equilibrium constant (K_B) of pure phenoxy.[32] Therefore, it seems that the value of σ_e is dependent on the relative ratio of K_A versus K_B according to the Painter–Coleman association model. Detailed results will be discussed in the future concerning the effect of the hydrogen-bonding strength on σ_e.

q has been found to be one parameter most closely correlated to the molecular structure, and the most important contribution to its relative magnitude is probably the inherent stiffness of the chain itself. q can be derived from σ_e with the following relationship:[23]

$$q = 2\sigma_e A_0 \tag{6}$$

where A_0 is the cross-section area of the polymer blend. For PCL, A_0 is 0.186 nm^2.[26] Therefore, the value of q calculated in this study is 3.93 kcal/mol, which is close to that previously reported by DeJuana and Cortazar.[13] Polymers with very flexible chains, such as polyethers, have q values of about 3 kcal/mol, and polymers with intermediate flexibility, such as PE, have q values around 5 kcal/mol.[33] A polyester such as PCL has a lower T_m than PE, and this indicates that it possesses a very flexible polymer chain. Therefore, the q value of PCL in this work is considered reasonable.

Morphology

As mentioned previously in the introduction, the domain size of the PCL crystalline/amorphous phase is between 3 and 20 nm according to solid-state NMR analysis. However, the exact thickness of the crystalline phase in the phenolic/PCL blend is still unknown. In this study, the lamellar periodicities of these phenolic/PCL blends were determined with SAXS. Figure 9 shows the profiles of Lorentz-corrected intensities (Iq^2) of pure PCL and phenolic/PCL blends at T_c = 40 °C. The peak position shifts toward lower angles with increasing phenolic content, and this indicates that the long period increases with the increase in the phenolic content according to Bragg's law. This phenomenon may be due to the thickness of PCL crystals or the swelling of amorphous layers via blending with phenolic. Generally, the average thickness of a crystalline phase can be determined with a one-dimensional correlation func-

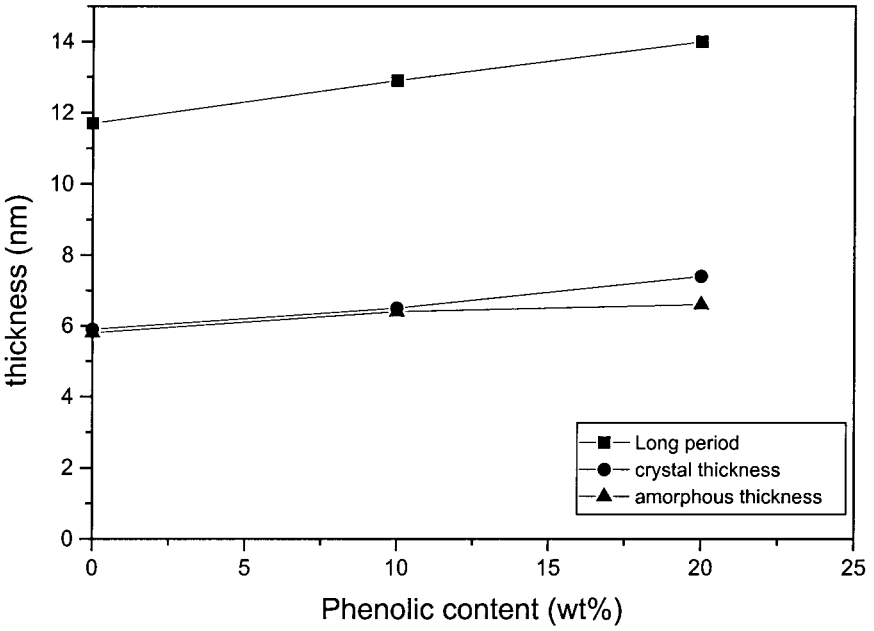

Figure 10. Composition variations of the long period and the thickness of amorphous and crystalline phases.

tion. This one-dimensional correlation function is defined as follows:[34]

$$r(z) = \frac{1}{r(0)} \int_0^\infty I(q) q^2 \cos(qz) dq \tag{7}$$

where z is the correlation distance and $r(0)$ is the scattering invariant. Because the experimentally accessible q range is finite, the extrapolation of the intensity to low and high q values is necessary for the integrations. Extrapolation to zero q is used by the Debye–Bueche model:[35,36]

$$I(q) = \frac{A}{(1 + a_c^2 q^2)^2} \tag{8}$$

where A is a constant and a_c is the correlation length. A and a_c can be obtained from the slope of $I(q)^{-1/2}$ versus q^2 with the intensity data at a low-q region. The large q value can be determined with the Porod–Ruland model:[37]

$$I(q) = K_p \frac{\exp(-\sigma^2 q^2)}{q^4} + I_{fl} \tag{9}$$

where K_p is the Porod constant, σ is a parameter related to the thickness of the crystal/amorphous interphase, and I_{fl} is the back-group intensity from thermal density fluctuations. These values were obtained by the curve fitting of the intensity profile at a high-q region. Therefore, the values of the thickness of the crystalline phase and amorphous phase can be obtained with the one-dimension correlation function. Figure 10 displays the changes in the thickness of the crystalline phase and amorphous phase in phenolic/PCL blends, showing that the crystal and amorphous thickness increases with the phenolic content. The values are consistent with the previous solid-state NMR analysis showing that the crystal thickness is less than 20 nm and larger than 3 nm. The same trend of increasing crystal and amorphous thickness was also found in a poly(styrene-*co*-vinyl phenol)/PEO blend system.[10] The effect of blending on the crystal thickness has been studied for many systems. In most blend systems, the reduction of crystal thickness has been found in weakly interacting blends such as poly(vinyl chloride) (PVC)/PCL[38] and poly(styrene-*co*-acrylonitrile)/PCL.[39] On the contrary, an increase in thickness has been observed in strongly hydrogen-bonding interaction systems such as poly(vinyl phenol)/PCL[40] and poly(styrene-*co*-vinyl phenol)/PEO blends. According to the secondary nu-

cleation theory, the initial crystal thickness is given by[41,42]

$$\lg^* \cong \frac{2\sigma_e T_m^0}{\Delta h_f^0 (T_m^0 - T_c)} \quad (10)$$

In general, the formation of thicker crystals in a blend is attributed to the depression of T_m^0 because the initial crystal is inversely proportional to the degree of supercooling in eq 10. The depression of T_m^0 by blending lowers the degree of supercooling for a given T_c, and a large lg* is induced in the blend. It is well known that the depression of T_m^0 is found in most miscible systems, which reduces the formation of thicker crystals. However, as mentioned previously, a reduction of crystal thickness has been found in PVC/PCL and poly(styrene-co-acrylonitrile) (SAN)/PCL. It is clear now that the initial crystal thickness is not only dependent on the degree of supercooling but is also dependent on σ_e in eq 10. The reduction of σ_e was found in PVC/PCL and SAN/PCL blend systems;[12] therefore, the thickness of the crystalline phase decreases with an increase in PVC and SAN contents. In this work, σ_e for phenolic/PCL blends increases with increasing phenolic content. As a result, the thickness of the crystalline phase increases with the increase of the phenolic content because of the increasing σ_e value and reduces the degree of supercooling based on eq 10. We confirm here that the thickness of the crystalline phase is also strongly dependent on σ_e. Here, an interesting question is raised: can we establish a general principle for predicting the thickness of crystals in miscible polymer blends? Detailed results will be discussed further in the future.

CONCLUSIONS

The quantitative analyses of the crystallization kinetics, σ_e, and morphology in phenolic/PCL binary blends have been investigated. The crystallization behavior of PCL from the melt is strongly influenced by the composition and T_c. The addition of the phenolic component to PCL causes a depression in both the overall crystallization rate and T_m. In addition, the presence of the amorphous phenolic component results in a reduction in the spherulite growth rate of PCL according to the Lauritzen–Hoffman model. Both the nucleation constant and σ_e of PCL increase with an increase in the phenolic content, and this indicates that the crystallization ability of PCL decreases with increasing phenolic content in the blends. The SAXS data show that the crystal thickness of the phenolic/PCL blend is greater than that of pure PCL because of the increase in σ_e and the decrease in the degree of supercooling. The observed domain size of the crystalline/amorphous phase from SAXS data is also consistent with that from solid-state NMR. A detailed principle for predicting the thickness of crystals in miscible blends will be examined in the future.

The authors thank the National Science Council of Taiwan for financially supporting this research (NSC-91-2216-E-009-018). They are also grateful to Tsang-Lang Lin of the Department of Engineering and System Science at National Tsing Hua University for assistance with the SAXS measurements.

REFERENCES AND NOTES

1. Wang, T. T.; Nishi, T. Macromolecules 1977, 10, 421.
2. Amelino, L.; Martuscelli, E.; Sellitti, C.; Silvestre, C. Polymer 1990, 31, 1051.
3. Alfonso, G. C.; Russell, T. P. Macromolecules 1986, 19, 1143.
4. Russell, T. P.; Ito, H.; Wignall, G. D. Macromolecules 1988, 21, 1073.
5. Crevecoeur, G.; Grenninckx, G. Macromolecules 1991, 24, 1190.
6. Runt, J.; Miley, D. M.; Zhang, X.; Gallagher, K. P.; McFeaters, K.; Fishburn, J. Macromolecules 1992, 25, 1929.
7. Martuscelli, E.; Pracella, M. Polymer 1984, 25, 1097.
8. Zemel, I. S.; Roland, C. M. Polymer 1992, 33, 3427.
9. Runt, J. In Polymer Blends; Paul, D. R., Ed.; Wiley: New York, 2000; Vol. 1.
10. Talibuddin, S.; Wu, L.; Runt, J.; Lin, J. S. Macromolecules 1996, 29, 7527.
11. Xing, P.; Ai, X.; Dong, L.; Feng, Z. Macromolecules 1998, 31, 6898.
12. Eastmond, G. C. Adv Polym Sci 1999, 149, 223.
13. DeJuana, R.; Cortazar, M. Macromolecules 1993, 26, 1170.
14. Kuo, S. W.; Chang, F. C. Macromol Chem Phys 2001, 201, 3112.
15. Nishi, T.; Wang, T. T. Macromolecules 1975, 8, 909.
16. Coleman, M. M.; Graf, J. F.; Painter, P. C. Specific Interactions and the Miscibility of Polymer Blends; Technomic: Lancaster, PA, 1991.
17. Zhong, Z.; Guo, Q.; Mi, Y. Polymer 1998, 40, 27.
18. Avrami, M. J. Chem Phys 1939, 7, 1103.
19. Wang, T. T.; Nishi, T. Macromolecules 1977, 10, 4219.

20. Wang, Z.; Jiang, B. Macromolecules 1997, 30, 6223.
21. An, Y.; Dong, L.; Li, G.; Mo, Z.; Feng, Z. J Polym Sci Part B: Polym Phys 2000, 38, 1860.
22. DeJuana, R.; Cortazai, M. Macromolecules 1994, 27, 50.
23. Hoffman, J. D.; Davis, G. T.; Lauritzen, J. I., Jr. In Treatise on Solid State Chemistry; Hannay, N. B., Ed.; New York: Plenum, 1976; Vol. 3.
24. Williams, M. L.; Landel, R. F.; Ferry, J. D. J Am Chem Soc 1975, 77, 3701.
25. Hoffman, J. D. Polymer 1983, 24, 3.
26. Phillips, P. J.; Rensch, G. J.; Taylor, K. D. J Polym Sci Part B: Polym Phys 1987, 25, 1725.
27. Crescenzi, V.; Manzini, G.; Calzolari, G.; Borri, C. Eur Polym J 1972, 8, 449.
28. Thomas, D. G.; Staveley, L. A. K. J Chem Soc 1952, 4569.
29. Rotiman, D. B.; Marand, H.; Miller, R. L.; Hoffman, J. D. J Phys Chem 1989, 93, 6919.
30. Zhong, Z.; Guo, Q. Polymer 2000, 41, 1711.
31. Kuo, S. W.; Lin, C. L.; Chang, F. C. Macromolecules 2002, 35, 278.
32. Iriarte, M.; Alberdi, M.; Shenoy, S. L.; Iruin, J. J. Macromolecules 1999, 32, 2661.
33. Hoffman, J. D.; Miller, R. L.; Marand, H.; Rotiman, D. B. Macromolecules 1992, 25, 2221.
34. Strobl, G. R.; Schneider, M. J Polym Sci Polym Phys Ed 1980, 18, 1343.
35. Debye, P.; Bueche, A. M. J Appl Phys 1949, 20, 518.
36. Debye, P.; Anderson, Jr. H. R.; Brumberger, H. J Appl Phys 1957, 28, 679.
37. Ruland, W. J. J Appl Crystallogr 1971, 4, 70.
38. Chen, H. L.; Li, L. J.; Lin, T. L. Macromolecules 1998, 31, 2255.
39. Runt, J. P.; Zhang, X.; Miley, D. M.; Gallagher, K. P.; Zhang, A. Macromolecules 1992, 25, 3902.
40. Chen, H. L.; Wang, S. F.; Lin, T. L. Macromolecules 1998, 31, 8924.
41. Hoffman, J. D.; Weeks, J. J. J Res Natl Bur Stand Sect A 1962, 66, 13.
42. Hoffman, J. D.; Miller, R. L. Polymer 1997, 38, 3151.